Relativistic effects in hydrogenlike atoms embedded in Debye plasmas

D. Bielińska-Wąż and J. Karwowski
Instytut Fizyki, Uniwersytet Mikołaja Kopernika, ul. Grudziądzka 5, PL-87-100 Toruń, Poland

B. Saha and P. K. Mukherjee
Department of Spectroscopy, Indian Association for the Cultivation of Science, Jadavpur, Kolkata 700 032, India
(Received 2 June 2003; published 28 January 2004)

Spectra of hydrogenlike atoms embedded in a Debye plasma are investigated. The state energies and the transition rates are studied using a fully relativistic formalism based on the Dirac equation. The effect of the plasma is described by introducing an exponential screening to the nuclear Coulomb potential (the Debye screening). Systematic trends with respect to both the nuclear charge and the screening parameter are observed for all calculated quantities. The pattern of splittings of $ns_{1/2}$, $np_{1/2}$ and $np_{3/2}$ is modified in a specific way due to the combined relativity and plasma effect. The transition rates decrease with an increase of the Debye parameter as well as with an increase of Z.

DOI: 10.1103/PhysRevE.69.016404 PACS number(s): 52.25.Os, 31.30.Jv, 31.15.Ar, 03.65.Ge

I. INTRODUCTION

Studies of the spectral properties of ionized atoms embedded in plasma are important not only for plasma diagnostics but also for understanding stellar spectra and atmospheric opacities. The effect of a plasma may be conveniently described by an exponential screening potential, known in plasma physics as the *Debye* or *Debye-Hückel potential* [1–4]. The same potential appears in several other areas of physics. In particular, in nuclear physics it is known as the *Yukawa potential* and in solid-state physics it is called the *Thomas-Fermi potential*. Consequently, the relevance of studies of the spectra of quantum systems in which interactions are governed by this kind of potential extends far beyond the plasma physics. Many interesting results as well as references to other works on this subject may be found in Refs. [5–8]. Also the we have contributed to this area of research [9–12]. However, all the works we are familiar with are concerned with nonrelativistic descriptions of the spectra of Debye-screened atoms. The effects of the plasma strength, of the electron correlation, and of the degree of ionization were studied in detail and, at least for small Debye-screened atoms, are already rather well understood. On the contrary, the influence of relativistic effects, though expected to be important (particularly for highly ionized species), has hardly been mentioned in the literature. The present study is aimed at filling in this gap. We investigate the influence of relativistic effects on the spectra of Debye-screened hydrogenlike atoms. The corresponding Dirac equation is solved numerically for a range of Debye parameters and for a number of nuclear charge values. The present study is concerned with the ground states and two lowest excited states of $^2S_{1/2}$, $^2P_{3/2}$, and $^2P_{1/2}$ symmetries. The theoretical model is outlined in Sec. II while the results are discussed in Sec. III. Hartree atomic units are used throughout this paper.

II. THE MODEL

The Debye potential describing the interaction between the nuclear charge Z and an electron is given by

$$V_\mu(r) = -\frac{Z e^{-\mu r}}{r}, \tag{1}$$

where μ is the Debye-screening parameter. For a hydrogenlike atom the corresponding radial Schrödinger equation is

$$\left[-\frac{1}{2}\frac{d^2}{dr^2} + \frac{l(l+1)}{2r^2} - \frac{Z e^{-\mu r}}{r} - E_{nl}(Z,\mu)\right] R_{nl}(Z,\mu;r) = 0. \tag{2}$$

Upon making the substitution

$$\rho = Zr \tag{3}$$

Eq. (2) becomes

$$\left[-\frac{1}{2}\frac{d^2}{d\rho^2} + \frac{l(l+1)}{2\rho^2} - \frac{e^{-\lambda\rho}}{\rho} - \varepsilon_{nl}(\lambda)\right] R_{nl}(1,\lambda;\rho) = 0, \tag{4}$$

where

$$\lambda = \mu/Z \tag{5}$$

and

$$\varepsilon_{nl}(\lambda) = E_{nl}(Z,\mu)/Z^2 = E_{nl}(1,\lambda). \tag{6}$$

The normalization of the radial functions

$$\int_0^\infty |R_{nl}(Z,\mu;r)|^2 dr = \int_0^\infty |R_{nl}(1,\lambda;\rho)|^2 d\rho = 1, \tag{7}$$

and Eqs. (2) and (4) imply that

$$\langle R_{nl}(Z,\mu;r)|r^k|R_{n'l'}(Z,\mu;r)\rangle = Z^{-k}\langle R_{nl}(1,\lambda;r)|r^k|R_{n'l'}(1,\lambda;r)\rangle. \tag{8}$$

Relation (6) between the energy levels and relation (8) between the matrix elements lead to the derivation of the spectral properties of an arbitrary one-electron ion from the cor-

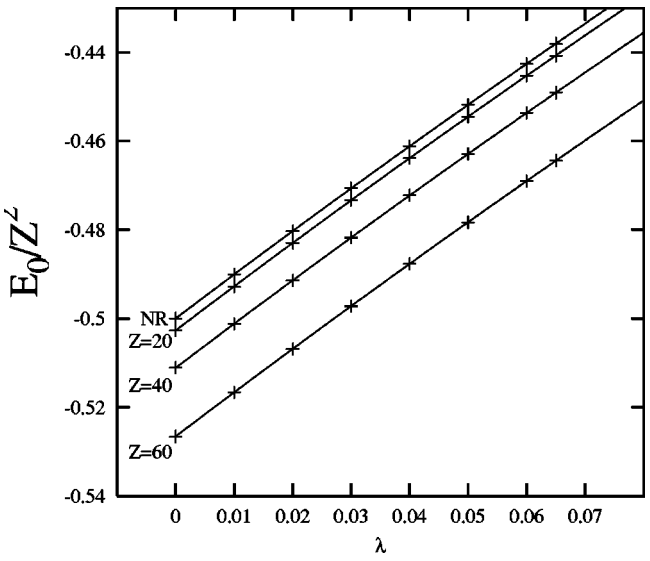

FIG. 1. Scaled ground state energies $E_0/Z^2 \equiv \varepsilon_{1s_{1/2}}$ against the screening parameter λ for several values of Z. The nonrelativistic values of ε_{1s} are Z independent and, up to the width of the line, overlap with the relativistic $Z=1$ ones. All quantities are in atomic units.

responding properties of the hydrogen atom with a properly scaled [Eq. (5)] Debye-screening parameter.

Alternatively, Eq. (4) may be rewritten as

$$[H_0 + V'_\lambda - \varepsilon_{nl}(\lambda)] R_{nl}(1,\lambda;\rho) = 0, \tag{9}$$

where H_0 is the Hamiltonian of a free hydrogenlike atom and

$$V'_\lambda = \frac{1-e^{-\lambda\rho}}{\rho} \tag{10}$$

is the perturbation due to the Debye screening. If $\lambda \ll 1$, as it is in majority of realistic plasmas, the perturbation is small and the first-order corrections may give an adequate estimate of the shift of the energy levels. Thus, up to the first order of perturbation theory, the energy may be written as

$$\varepsilon_{nl}(\lambda) = \varepsilon_{nl}(0) + J_0^{(nl)} - J_\lambda^{(nl)}, \tag{11}$$

where $\varepsilon_{nl}(0)$ is the eigenvalue of H_0 and

$$J_\lambda^{(nl)} = \langle R_{nl}(1,0;\rho) | e^{-\lambda\rho}/\rho | R_{nl}(1,0;\rho) \rangle. \tag{12}$$

Using the explicit form of the eigenfunctions of H_0, i.e., of $R_{nl}(1,0;\rho)$, one can easily evaluate the perturbative correction with

$$J_\lambda^{(nl)} = \frac{1}{n^2} \binom{n+l}{k} \frac{(n\lambda/2)^{2k}}{(n\lambda/2+1)^{2n}} F(-k,-k,2l+2,x), \tag{13}$$

where $k = n-l-1$, $x = 2/(n\lambda)^2$, and F is the Gauss hypergeometric function [13]. In particular,

$$J_0^{(nl)} = 1/n^2, \tag{14}$$

$$J_\lambda^{(n,n-1)} = \frac{1}{n^2(n\lambda/2+1)^{2n}}, \tag{15}$$

and

$$J_\lambda^{(n,n-2)} = \frac{1+n^2(n-1)\lambda^2/2}{n^2(n\lambda/2+1)^{2n}}. \tag{16}$$

A similar analysis may be performed for atoms described by either the Dirac (in the one-electron case) or by the Dirac-Coulomb (in the many-electron case) equation. The radial Dirac equation for a hydrogenlike atom is

$$\begin{pmatrix} -\frac{Z e^{-\mu r}}{r} - E_{nlj}(Z,\mu) & c\left(\frac{\kappa}{r} - \frac{d}{dr}\right) \\ c\left(\frac{\kappa}{r} + \frac{d}{dr}\right) & -\frac{Z e^{-\mu r}}{r} - 2c^2 - E_{nlj}(Z,\mu) \end{pmatrix} \times \begin{pmatrix} R^L_{nlj}(Z,\mu;r) \\ R^S_{nlj}(Z,\mu;r) \end{pmatrix} = 0, \tag{17}$$

where $\kappa = \pm(j+\frac{1}{2})$ for $\ell = j \pm \frac{1}{2}$ is the Dirac angular momentum quantum number, $R^L_{nlj}(Z,\mu;r)$ and $R^S_{nlj}(Z,\mu;r)$ are the radial parts of the large and small components of the wave function, respectively, $E_{nlj}(Z,\mu)$ is the energy relative to c^2 (the rest energy of electron), and the remaining symbols have their usual meaning. The scaling, Eq. (3), and the substitution of Eq. (5) results in the equation

$$\begin{pmatrix} -\frac{e^{-\lambda\rho}}{\rho} - \varepsilon_{nlj}(\zeta,\lambda) & \frac{1}{\zeta}\left(\frac{\kappa}{\rho} - \frac{d}{d\rho}\right) \\ \frac{1}{\zeta}\left(\frac{\kappa}{\rho} + \frac{d}{d\rho}\right) & -\frac{e^{-\lambda\rho}}{\rho} - \frac{2}{\zeta^2} - \varepsilon_{nlj}(\zeta,\lambda) \end{pmatrix} \times \begin{pmatrix} R^L_{nlj}(\zeta,\lambda;\rho) \\ R^S_{nlj}(\zeta,\lambda;\rho) \end{pmatrix} = 0, \tag{18}$$

where $\zeta = Z/c$ and $\varepsilon_{nlj} = E_{nlj}/Z^2$. Equation (18), similar to Eq. (17), depends on two parameters. However, from Eq. (18) one can clearly see that the relativistic effect (i.e., the c-dependent contributions) are determined, as in the case of a free atom, by the ratio Z/c only. As one can easily note, contrary to the nonrelativistic case, $Z=1$ results do not determine their counterparts for larger values of Z.

The perturbative corrections to the relativistic energies may also be determined in a way similar to that in the nonrelativistic theory. Then,

$$\begin{aligned} \varepsilon_{nlj}(\zeta,\lambda) &= \varepsilon_{nlj}(\zeta,0) + \mathcal{J}_0^{(nlj)} - \mathcal{J}_\lambda^{(nlj)} \\ &= \varepsilon_{nlj}(\zeta,0) - \Delta_{nlj}(\zeta,\lambda) + \mathcal{O}(\lambda^3), \end{aligned} \tag{19}$$

where $\varepsilon_{nlj}(\zeta,0)$ is the Dirac energy of a free atom,

$$\mathcal{J}_\lambda^{(nlj)} = \langle e^{-\lambda\rho}/\rho \rangle, \tag{20}$$

$$\Delta_{nlj}(\zeta,\lambda) = -\lambda + \tfrac{1}{2}\lambda^2 \langle \rho \rangle, \tag{21}$$

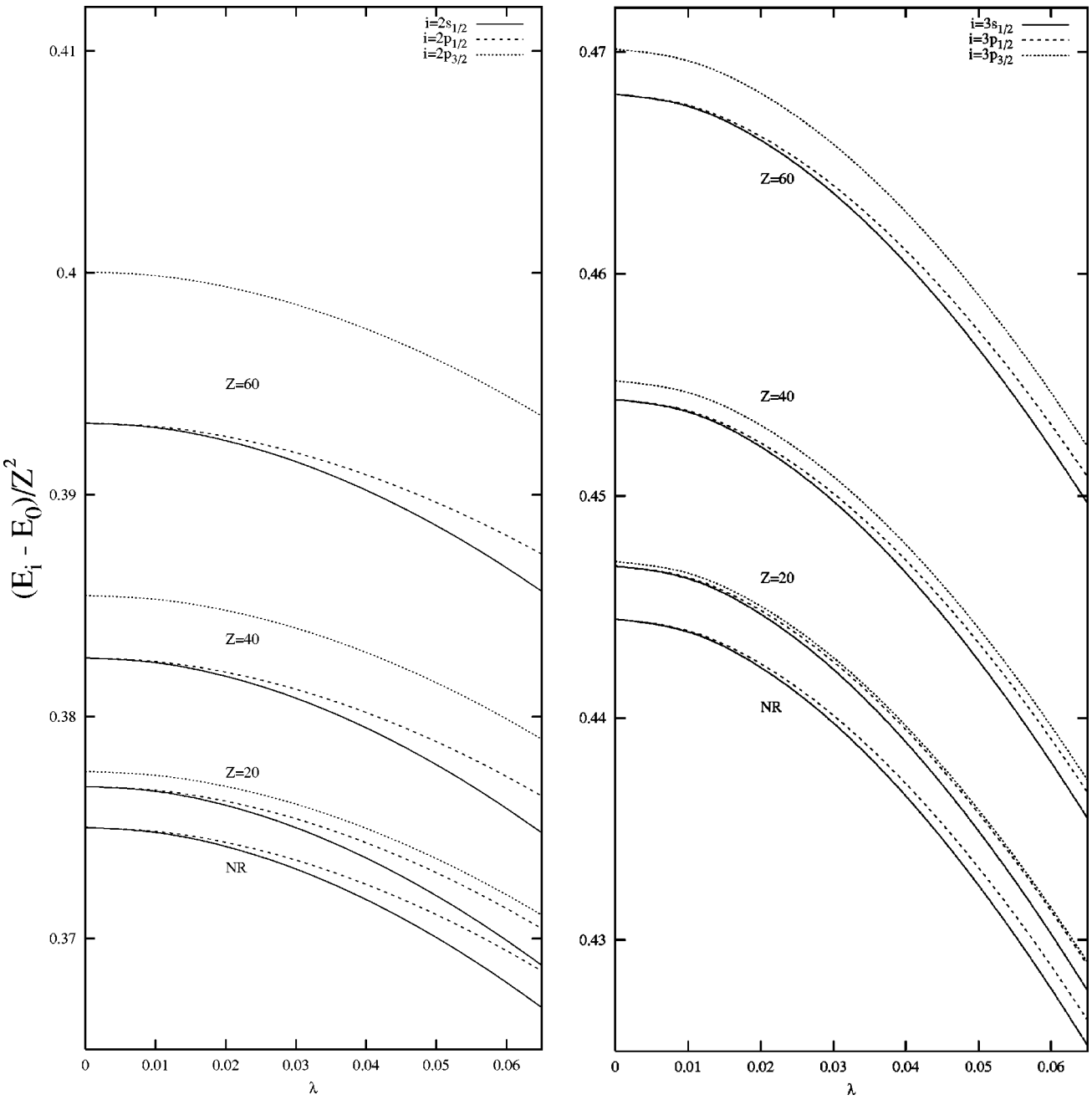

FIG. 2. Excitation energies, scaled by Z^{-2}, for $Z=1,20,40,60$, against λ. The lowest curves correspond to the nonrelativistic case and (up to the thickness of the lines) to the relativistic $Z=1$ case. The consecutive groups of curves correspond to $Z=20$, $Z=40$, and $Z=60$. All quantities are in atomic units.

and

$$\langle\Omega\rangle=\langle R^L_{nlj}(\zeta,0;\rho)|\Omega|R^L_{nlj}(\zeta,0;\rho)\rangle + \langle R^S_{nlj}(\zeta,0;\rho)|\Omega|R^S_{nlj}(\zeta,0;\rho)\rangle, \quad (22)$$

where Ω is a scalar operator.

The general formulas for $\mathcal{J}^{(nlj)}_\lambda$ are rather cumbersome. However, for our purposes it is sufficient to use much simpler expressions for several special cases and for the expectation values of several powers of $\langle\rho\rangle$ [14,15]. In particular,

$$\Delta_{nlj}(\zeta,\lambda)=-\lambda+\lambda^2[(3N_\kappa^2-\kappa^2)\tilde{n}_\kappa-\kappa N_\kappa]/(4N_\kappa). \quad (23)$$

Here $N_\kappa=\sqrt{\tilde{n}_\kappa^2+\zeta^2}$, $\tilde{n}_\kappa=n_r+s_\kappa$, $n_r=n-|\kappa|$, and $s_\kappa=\sqrt{\kappa^2-\zeta^2}$. The explicit expressions for $\mathcal{J}^{(nlj)}_\lambda$, $n=1,2$ may easily be derived from the radial hydrogenic Dirac wave functions. Then,

$$\mathcal{J}^{(1,0,1/2)}_\lambda=[s_1(1+\lambda/2)^{2s_1}]^{-1},$$

$$\mathcal{J}^{(2,1,3/2)}_\lambda=[2s_2(1+\lambda)^{2s_2}]^{-1},$$

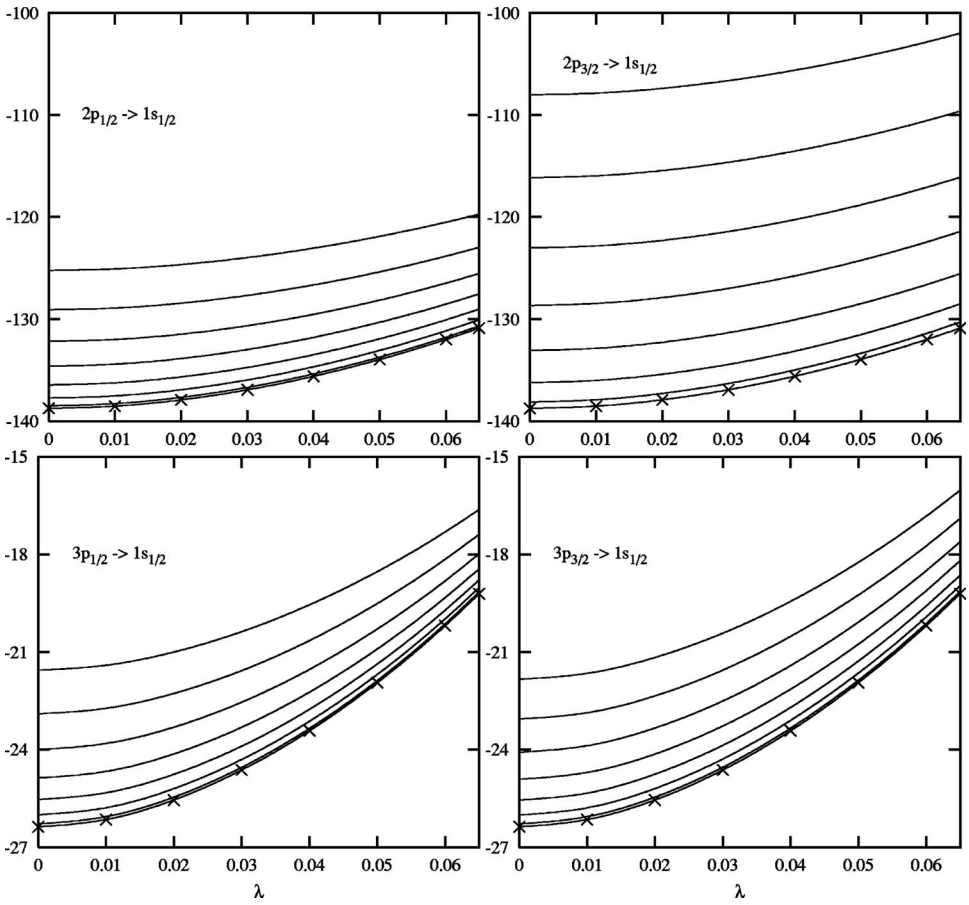

FIG. 3. Oscillator strengths corresponding to $np_j \rightarrow 1s_{1/2}$ transitions divided by $2j+1$ and multiplied by 10^3. The lowest curves correspond to the nonrelativistic case and (up to the width of the lines) to the relativistic $Z=1$ case. The consecutive curves correspond to $Z=10$, 20, 30, 40, 50, 60, 70.

$$\mathcal{J}_\lambda^{(2,0,1/2)}=[1-\lambda N_2(N_2^2-4)/2+\lambda^2 N_2(N_2-1)\times(N_2+2)/4]/A,$$

$$\mathcal{J}_\lambda^{(2,1,1/2)}=[1-\lambda N_2(N_2^2-4)/2-\lambda^2 N_2(N_2+1)\times(N_2-2)/4]/A, \quad (24)$$

where $A=N_2(N_2^2-2)(1+\lambda N_2/2)^{N_2^2}$. Similarly [14,15]

$$\mathcal{J}_0^{(nlj)}=(n_r+\kappa^2/s_\kappa)/N_\kappa^3. \quad (25)$$

As one can see from Eq. (23),

$$\varepsilon_{n,l+1,j}-\varepsilon_{n,l,j}=|\kappa|\lambda^2/2+O(\lambda^3). \quad (26)$$

In particular,

$$\varepsilon_{2p_{1/2}}-\varepsilon_{2s_{1/2}}=\tfrac{1}{2}\lambda^2(1+\lambda N_2)^{-N_2}. \quad (27)$$

Hence, the states which differ by the sign of κ only, degenerate in a free Dirac atom, are split due to the Debye screening. The splitting is proportional to λ^2, and the energy of the state with the lower orbital angular momentum is always lower.

III. RESULTS AND DISCUSSION

The eigenvalue equations (4) and (18) have been solved numerically. The accuracy of the integration procedure has been chosen to assure that the resulting energies are correct to 1 millihartree. The calculations have been performed for $0 \leqslant \lambda < 0.065$. The largest value of λ corresponds to the limit of stability of a nonrelativistic hydrogenlike atom in its $4p$ configuration. The calculated quantities include: ground state energies (Fig. 1), excitation energies (Fig. 2) and emission oscillator strengths (Fig. 3). All quantities are plotted against λ for several values of Z ranging from 1 to 70.

The scaled nonrelativistic ground state energies ε_{nl} and the relativistic ones ε_{nlj} are displayed in Fig. 1. The nonrelativistic energies do not depend on Z and are represented by the highest line in the figure. The consecutive lines correspond to the relativistic energies for $Z=20,40,60$. The dependence on λ is, for $\lambda \ll 1$, dominated by the linear term. For larger λ, the departure from linearity becomes considerable and the slope of the corresponding curves gradually decreases, as can be seen from Eqs. (19), (20), and (24). A similar behavior of the total energies appears also in the nonrelativistic models [9–11]. The relativistic effects, described by the Z dependence of the scaled energies, as one should expect, grow increasingly fast with Z.

The excitation energies scaled by $1/Z^2$ are plotted against λ in Fig. 2. Here again the nonrelativistic values of $\varepsilon_{nl}-\varepsilon_{1s}$ are Z independent. They are represented by the two lowest curves (the solid curves correspond to the transitions to $l=0$ and the dotted ones to $l=1$ states). The splitting between these energy levels increases with increasing λ. The relativistic excitation energies are shown for $Z=20,40,60$.

TABLE I. Comparison of the exact $1s_{1/2} \rightarrow 2l_j$ excitation energies $\Delta\varepsilon_{nlj} = \varepsilon_{nlj} - \varepsilon_{1s_{1/2}}$ with the ones obtained using the first-order perturbation corrections; nr stands for *nonrelativistic* and δ is the difference between the exact and the perturbational energy. Energies are in millihartrees and λ in bohr^{-1}.

Z	λ	$\Delta\varepsilon_{2s_{1/2}}$	δ	$\Delta\varepsilon_{2p_{1/2}}$	δ	$\Delta\varepsilon_{2p_{3/2}}$	δ
nr	0.000	375.000	0.000	375.000	0.000	375.000	0.000
	0.010	374.781	0.000	374.829	0.000	374.829	0.000
	0.020	374.148	−0.002	374.333	−0.002	374.333	−0.002
	0.030	373.130	−0.010	373.531	−0.009	373.531	−0.009
	0.040	371.755	−0.029	372.440	−0.028	372.440	−0.027
	0.050	370.045	−0.065	371.076	−0.063	371.076	−0.063
	0.060	368.021	−0.125	369.450	−0.122	369.450	−0.122
	0.065	366.898	−0.166	368.543	−0.163	368.543	−0.163
20	0.000	376.850	0.000	376.850	0.000	377.524	0.000
	0.010	376.633	0.000	376.681	0.000	377.354	0.000
	0.020	376.004	−0.002	376.189	−0.002	376.857	−0.002
	0.030	374.994	−0.010	375.395	−0.009	376.055	−0.009
	0.040	373.629	−0.028	374.315	−0.027	374.964	−0.027
	0.050	371.931	−0.064	372.963	−0.062	373.599	−0.063
	0.060	369.921	−0.123	371.352	−0.121	371.973	−0.121
	0.065	368.804	−0.164	370.453	−0.161	371.065	−0.162
40	0.000	382.644	0.000	382.644	0.000	385.457	0.000
	0.010	382.432	0.000	382.480	0.000	385.286	0.000
	0.020	381.818	−0.002	382.004	−0.001	384.789	−0.002
	0.030	380.831	−0.009	381.233	−0.009	383.986	−0.009
	0.040	379.496	−0.027	380.184	−0.026	382.894	−0.027
	0.050	377.834	−0.062	378.871	−0.060	381.527	−0.062
	0.060	375.865	−0.119	377.305	−0.116	379.897	−0.122
	0.065	374.771	−0.159	376.430	−0.155	378.987	−0.161
60	0.000	393.229	0.000	393.229	0.000	400.044	0.000
	0.010	393.027	0.000	393.075	0.000	399.873	0.000
	0.020	392.438	−0.002	392.624	−0.002	399.375	−0.002
	0.030	391.490	−0.009	391.894	−0.008	398.570	−0.009
	0.040	390.207	−0.025	390.900	−0.024	397.475	−0.027
	0.050	388.608	−0.058	389.654	−0.055	396.103	−0.062
	0.060	386.712	−0.111	388.166	−0.107	394.468	−0.120
	0.065	385.657	−0.148	387.334	−0.144	393.554	−0.161

Splittings between $s_{1/2}$ and $p_{1/2}$ states increase as λ^2 [cf., Eqs. (26) and (27)]. In the first approximation these splittings are Z independent. It is interesting to note that the fine-structure splittings between states of the same l decrease with increasing λ.

A comparison between the exact energies and their approximate, first-order perturbation values, are given in Fig. 1 (total energies) and in Table I (excitation energies). As one can see, in the range of λ explored in this work, the perturbational energies are very close to the exact ones and their accuracy is adequate for spectroscopic studies of atoms embedded in plasmas. The difference δ between the exact and the perturbational energies corresponding to $1s_{1/2} \rightarrow 2l_j$ transitions, shown in Table I, never exceed 0.05%.

Emission oscillator strengths (multiplied by 1000 and divided by $2j+1$) for transitions from $np_{1/2}$ and $np_{3/2}$, $n=2,3$, to the ground state are plotted against λ in Fig. 3. The nonrelativistic oscillator strengths are Z independent and are represented by the lowest curves. The relativistic ones are represented by the consecutive curves and correspond, consecutively, to $Z=10,20,30,40,50,60,70$. The systematic trends and the importance of relativistic effects are clearly seen from the figure.

The results obtained show that for a correct interpretation of the spectra of ionized atoms in plasmas inclusion of relativistic effects is necessary, particularly for higher degrees of ionization. The behavior of excitation energies and transition rates as functions of the plasma strength and of the degree of ionization are regular. The first-order perturbation theory gives a very good approximation of the locations of the energy levels. Consequently, for an approximate description of the spectra the formulas derived from the perturbational expressions are quite adequate.

ACKNOWLEDGMENTS

This research was supported by the program of Indo-Polish Scientific and Technological Cooperation (Grant No. INT/POL/P-9/2000).

[1] G. Ecker and W. Weizel, Ann. Phys. (Leipzig) **17**, 126 (1956).
[2] H. Margenau and M. Lewis, Rev. Mod. Phys. **31**, 569 (1959).
[3] P. Winkler, Phys. Rev. E **53**, 5517 (1996).
[4] L. Zhang and P. Winkler, Int. J. Quantum Chem. **S30**, 431 (1996).
[5] J.P. Gazeau and A. Maquet, Phys. Rev. A **20**, 727 (1979).
[6] Z. Wang and P. Winkler, Phys. Rev. A **52**, 216 (1995).
[7] S.-T. Dai, A. Solovyova, and P. Winkler, Phys. Rev. E **64**, 016408 (2001).
[8] J.M. Ugalde, C. Sarasola, and X. Lopez, Phys. Rev. A **56**, 1642 (1997).
[9] P.K. Mukherjee, J. Karwowski, and G.H.F. Diercksen, Chem. Phys. Lett. **363**, 323 (2002).
[10] B. Saha, P.K. Mukherjee, and G.H.F. Diercksen, Astron. Astrophys. **396**, 337 (2002).
[11] B. Saha, T.K. Mukherjee, P.K. Mukherjee, and G.H.F. Diercksen, Theor. Chem. Acc. **108**, 305 (2002).
[12] B. Saha, P.K. Mukherjee, D. Bielińska-Wąż, and J. Karwowski, J. Quant. Spectrosc. Radiat. Transf. **78**, 131 (2003).
[13] *Handbook of Mathematical Functions*, edited by M. Abramowitz and I. A. Stegun (National Bureau of Standards, Washington, D.C., 1964), Chap. 15.
[14] J. Kobus, J. Karwowski, and W. Jaskólski, J. Phys. A **20**, 3347 (1987).
[15] D. Andrae, J. Phys. B **30**, 4435 (1997).